

Importance of conduction electron correlation in a Kondo lattice, Ce_2CoSi_3

Swapnil Patil, Sudhir Pandey, V. R. R. Medicherla, R. S. Singh, R. Bindu, E. V. Sampathkumaran and Kalobaran Maiti

Department of Condensed Matter Physics and Materials Science, Tata Institute of Fundamental Research, Homi Bhabha Road, Colaba, Mumbai - 400 005, INDIA.

E-mail: kbmaiti@tifr.res.in

Abstract.

Kondo systems are usually described by the interaction of strong correlation induced local moment with the highly itinerant conduction electrons. Here, we study the role of electron correlations among conduction electrons in the electronic structure of a Kondo lattice compound, Ce_2CoSi_3 , using high resolution photoemission spectroscopy and *ab initio* band structure calculations, where Co $3d$ electrons contribute in the conduction band. High energy resolution employed in the measurements helped to reveal signature of Ce $4f$ states derived Kondo resonance feature at the Fermi level and dominance of Co $3d$ contributions at higher binding energies in the conduction band. The line shape of the experimental Co $3d$ band is found to be significantly different from that obtained from the band structure calculations within the local density approximations, LDA. Consideration of electron-electron Coulomb repulsion, U among Co $3d$ electrons within the LDA+ U method leads to a better representation of experimental results. Signature of electron correlation induced satellite feature is also observed in the Co $2p$ core level spectrum. These results clearly demonstrate the importance of the electron correlation among conduction electrons in deriving the microscopic description of such Kondo systems.

PACS numbers: 75.20.Hr, 71.27.+a, 71.28.+d, 71.15.Mb

1. Introduction

Study of Ce-intermetallics have drawn significant attention during past few decades due to the observation of many unusual properties such as valence fluctuations, Kondo screening, heavy fermion superconductivity in these systems. Such properties arise due to the proximity of Ce $4f$ level to the Fermi level leading to strong hybridization between the Ce $4f$ states and the conduction electronic states [1]. Such hybridization often leads to a logarithmic enhancement of electrical resistivity at low temperatures in contrast to a decrease expected in a metal. This is known as Kondo effect. In the case of strong Kondo coupling, the antiparallel coupling of the Ce moment with the conduction electrons forms a singlet ground state called Kondo singlet that manifests as a sharp feature (Kondo resonance feature) in the electronic structure in the vicinity

of the Fermi level, ϵ_F . A lot of success has been achieved to describe these systems within the Anderson impurity models. Here, the parameters defining the hybridization between $4f$ states and valence electronic states are often estimated using band structure calculations based on local density approximations (LDA)[2, 3, 4, 5].

The scenario can be different if these materials contain transition metals: the d electrons forming the conduction band are strongly correlated. The finite correlation strength among them suggests non-applicability of the band structure results within LDA to derive the hybridization parameters and indicate the need to go beyond LDA prescriptions. A Kondo lattice compound, Ce_2CoSi_3 is a good candidate for this study. Ce_2CoSi_3 crystallizes in a AlB_2 derived hexagonal structure (space group $P6/mmm$) and is a mixed valent (Kondo lattice) compound [6, 7, 8]. The electrical transport measurements revealed temperature dependence[8] typical of a mixed valent system [9]. No signature of magnetic ordering was observed in the magnetic susceptibility measurements down to 0.5 K [8]. Interestingly, gradual substitution of Rh at Co sites leads to plethora of interesting features due to increasing dominance of indirect exchange interaction [8]. For example, $x = 0.6$ composition in $\text{Ce}_2\text{Rh}_{1-x}\text{Co}_x\text{Si}_3$ exhibits quantum critical behavior. Intermediate compositions having higher Rh concentration exhibit signature of spin density wave (SDW) state [8]. Clearly, the d electronic states corresponding to the transition metals plays a key role in determining the electronic properties in this interesting class of compounds. It is thus, important to probe the role of electron correlation in the electronic structure of these compounds.

In this paper, we report our results of investigation of the electronic structure of Ce_2CoSi_3 using high resolution photoemission spectroscopy and *ab initio* band structure calculations. High energy resolution employed in our measurements enabled us to reveal Kondo-resonance feature and the corresponding spin orbit satellite. The comparison of the experimental spectra and the calculated ones indicate that the correlation strength among Co $3d$ electrons is significant (~ 3 eV). The contribution of the Co $3d$ partial density of states (PDOS) is small in the vicinity of the Fermi level, where Ce $4f$ contributions are dominant.

2. Experimental details

Ce_2CoSi_3 was prepared by melting together stoichiometric amounts of high purity ($> 99.9\%$) Ce, Co and Si in an arc furnace. The single phase was confirmed by the absence of impurity peaks in the x -ray diffraction pattern. The specimen was further characterized by scanning electron microscopic measurements and energy dispersive x -ray analysis [8]. The photoemission measurements were performed using a Gammatdata Scienta SES2002 analyzer and monochromatic laboratory photon sources. The energy resolutions were set to 0.4 eV, 5 meV and 5 meV at Al $K\alpha$ (1486.6 eV), He $\text{II}\alpha$ (40.8 eV) and He $\text{I}\alpha$ (21.2 eV) photon energies, respectively. The base pressure in the vacuum chamber was 3×10^{-11} torr. The temperature variation down to 20 K was achieved by an open cycle He cryostat, LT-3M from Advanced Research Systems, USA. The sample surface was

cleaned by *in situ* scraping using a diamond file and the surface cleanliness was ensured by the absence of O 1s and C 1s features in the *x*-ray photoelectron (XP) spectra and the absence of impurity features in the binding energy range of 5-6 eV in the ultraviolet photoelectron (UP) spectra. The reproducibility of the spectra was confirmed after each trial of cleaning process.

3. Computational details

The electronic band structure of Ce_2CoSi_3 was calculated using *state-of-the-art* full potential linearized augmented plane wave (FLAPW) method using WIEN2k software[10] within the local density approximations, LDA. The convergence for different calculations were achieved considering 512 *k* points within the first Brillouin zone. The error bar for the energy convergence was set to < 0.2 meV per formula unit (fu). In every case, the charge convergence was achieved to be less than 10^{-3} electronic charge. The lattice constants used in these calculations are determined from the *x*-ray diffraction patterns considering AlB_2 derived hexagonal structure and are found to be $a = 8.104$ Å and $c = 4.197$ Å[6]. The muffin-tin radii (R_{MT}) for Ce, Co and Si were set to 2.5 a.u., 2.28 a.u. and 2.02 a.u., respectively.

4. Results and discussions

The valence band in Ce_2CoSi_3 consists of Ce 5*d*, Ce 4*f*, Co 3*d* and Si 3*p* electronic states. Since the transition probability of the photoelectrons in the photo-excitation process strongly depends on the excitation energies, a comparison of the photoemission spectra collected at different excitation energies would help to identify experimentally the character of various features constituting the valence band. In Fig. 1(a), we show the valence band spectra collected at 20 K using Al $K\alpha$ photon energy. The He $\Pi\alpha$ and He $\text{I}\alpha$ spectra are shown in Fig. 1(b). In order to compare the spectral functions, it is important to subtract suitable background from the raw data as shown in Fig. 2. We have subtracted integral background from Al $K\alpha$ and He Π spectra. Since the thermalized electrons lead to a large increase in background at low kinetic energies, the background function in the He I spectrum are often found to be better defined by a polynomial (quadratic like) as shown in Fig. 2(a). Evidently, the background contributions in the energy range 0 - 3 eV binding energies is quite small in every case. Moreover, different functional dependence of the background in the He I spectrum does not have significant influence on the conclusions as the calculated spectra are compared with the XP spectrum.

In Fig. 1(b), the intensity close to the Fermi level, ϵ_F , exhibit significantly different behavior as a function of excitation energy. He Π spectrum exhibits large intensity and two distinct features C and K near ϵ_F , which are not visible in the other spectra. The high energy resolution employed in the He I and He Π measurements helped to resolve distinct signature of the features in the vicinity of ϵ_F . The photoemission cross section

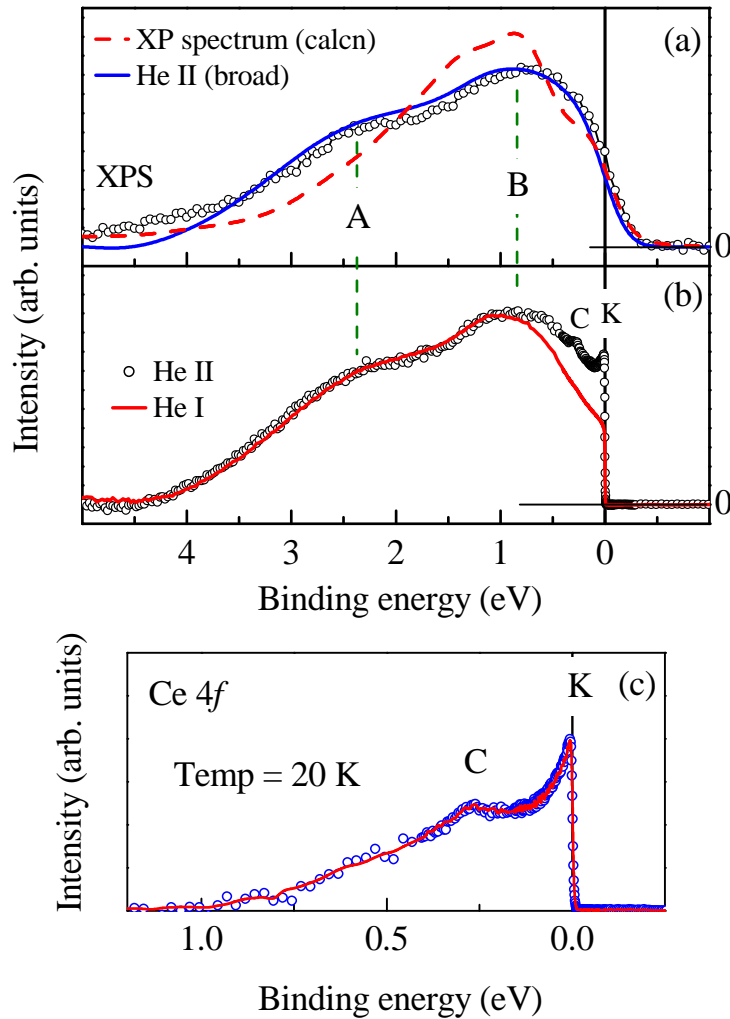


Figure 1. Valence band spectra collected using (a) Al $K\alpha$ (XPS), and (b) He II and He I excitation energies. The solid line in (a) represents the broadened He II spectrum to take into account the energy resolution corresponding to XP spectrum. Dashed line represent the calculated XP spectrum as described later in the text. (c) The Ce 4f spectral function obtained by subtracting He I spectrum from the He II spectrum.

for Ce 4f states at He II excitation energy is about 3 times larger than that at He I photon energy while it is almost the same for Si 3p states and double for Co 3d states [11]. Thus, the features C and K can be attributed to the photoemission signal primarily from the Ce 4f states. We have subtracted the He I spectrum from the He II spectrum to delineate the Ce 4f contributions. The subtracted spectrum representing Ce 4f band is shown in Fig. 1(c). The distinct features, C and K corresponding to the spin orbit satellite of the Abrikosov-Suhl resonance (ASR) and the main peak of ASR, respectively, could clearly be identified [17].

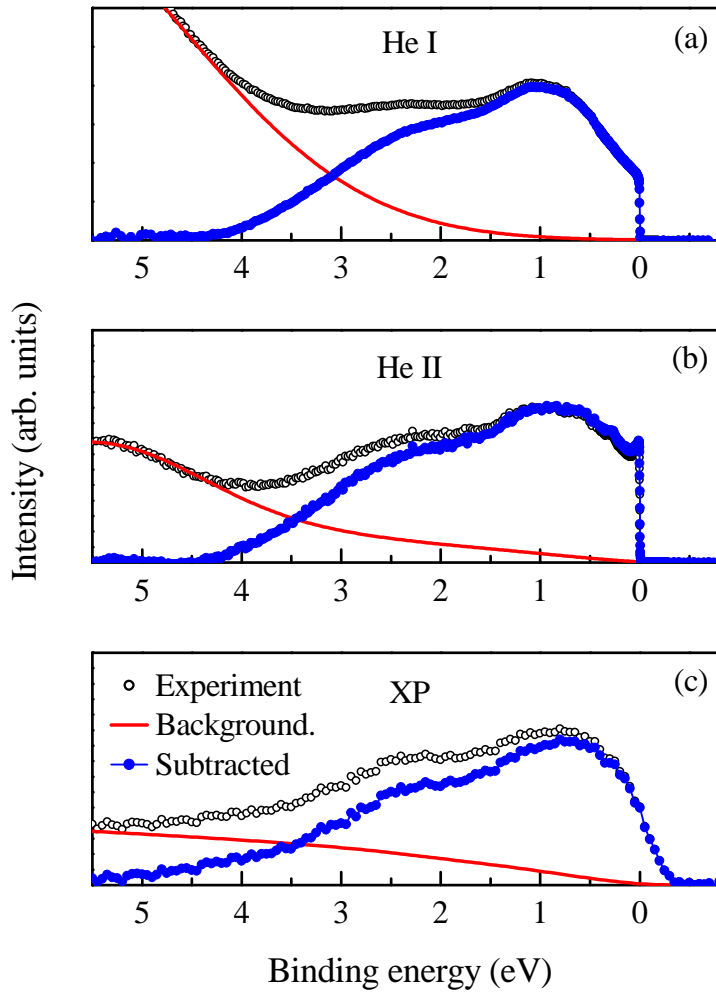


Figure 2. Background subtraction of the valence band spectra collected using (a) He I, (b) He II, and (c) Al $K\alpha$ excitation energies. The open circles represent raw data, lines represent the background function and the solid circles are the subtracted spectra.

In addition to the resonance feature at ϵ_F , each spectrum exhibits two distinct features, A and B at about 2.3 eV and 1 eV binding energies, respectively. Interestingly, the relative intensity of these features does not change with such a large change in photon energies. This is an important observation as the photoemission cross sections corresponding to Ce 5d, Ce 4f, Co 3d and Si 3p electronic states have significantly different excitation energy dependence [11]. To verify the change in lineshape with better clarity, we have broadened the He II spectrum by convoluting a Gaussian of full width at half maximum (FWHM) = 0.4 eV to make the resolution broadening comparable to that of the XP spectrum. The broadened spectrum is shown by solid line

superimposed over the XP spectrum in Fig. 1(a). The lineshapes of both the spectra are almost identical. In Fig. 1(b), the He I and He II spectra are superimposed over each other to investigate the change in lineshape when the energy resolution broadening is the same (~ 5 meV). The spectra in the binding energy range beyond 1 eV are found to be almost identical. All these observations are unusual.

These observations can not be associated to the surface preparation via scraping for the following reasons. Scraping helps to break the sample grains in a non-selective manner that helps to expose a clean surface for the measurements. In addition, scraping usually enhances the surface roughness. Such a process will enhance the surface contribution in the spectra. In addition, the linewidth of the features may also get enhanced due to scraping. This latter possibility can be ruled out as it is shown experimentally [12, 16] that cleaving and scraping have insignificant influence on the spectral lineshape at higher binding energies as the intrinsic linewidth of these features are already large due to various lifetime effects. As for the enhancement of surface contributions, it is already known that photoemission with He I and He II photons have significant surface sensitivity (probing depth is $\sim 8 - 10$ Å). Thus, these spectra may contain large surface contributions due to scraping. However, the Al $K\alpha$ valence band spectra possess dominant bulk contributions (probing depth ~ 25 Å). It is experimentally found that these spectra can often be considered as representative of the bulk electronic structure [12, 13, 14, 15] suggesting that the influence of scraping will have less influence in the Al $K\alpha$ spectrum. Thus, the observations of similar lineshape in the energy range of 1 to 3 eV binding energies in Figs. 1(a) and 1(b) suggest that either (i) the surface sensitivity in the He I and He II spectra are compensated by scraping or (ii) the surface and bulk electronic structures are quite similar and scraping has insignificant influence in the spectral lineshape. The former is unlikely as scraping enhances the surface contribution that will make the differences more prominent. Thus, the reasonable conclusion will be the latter case.

In order to verify the character of the features theoretically, we have calculated the electronic band structure using FPLAPW method. The calculated partial density of states (PDOS) are shown in Fig. 3. The dominant contribution in this energy range arises from the Ce $5d$, Ce $4f$, Co $3d$ and Si $3p$ PDOS as shown in Fig. 3(a), 3(b), 3(c) and 3(d) respectively. All the other contributions are negligible in this energy range. Evidently, Ce $5d$ contributions are small and almost equally distributed over the whole energy range shown. Ce $4f$ band is intense and narrow as expected. In order to provide clarity, we have rescaled the Ce $4f$ partial density of states (PDOS) by 25 times and shown by thick solid line in Fig. 3(b). The $4f$ PDOS contribute essentially in the vicinity of the Fermi level (< 1 eV binding energy). The intensity of Ce $4f$ band is significantly weak at higher binding energies. This is consistent with the observation in Fig. 1(b). Co $3d$ states also have finite contributions in this energy range due to the hybridization between Co $3d$ and Ce $4f$ states.

Co $3d$ and Si $3p$ electronic states are strongly hybridized and appear dominantly in the binding energy range larger than 0.5 eV. The bonding states contribute in

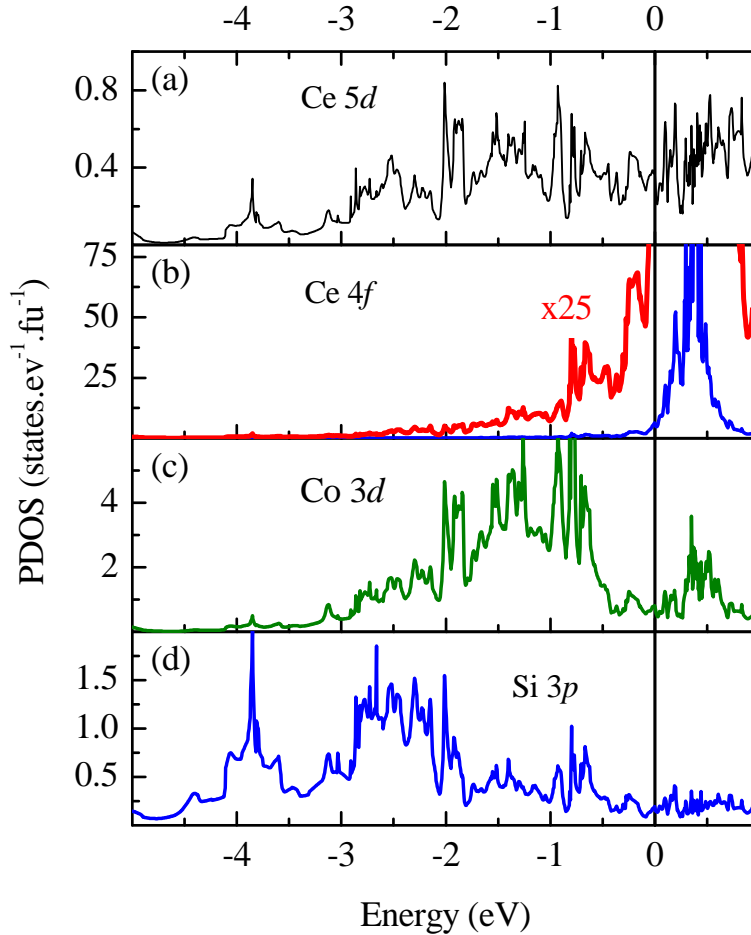


Figure 3. Calculated (a) Ce $5d$ partial density of states (PDOS), (b) Ce $4f$ PDOS, (c) Co $3d$ PDOS and (d) Si $3p$ PDOS. The thick solid line in (b) represents the Ce $4f$ PDOS rescaled by 25 times to show the weak intensities at lower energies.

the energy range higher than 2 eV binding energy, where the Si $3p$ PDOS has large contributions. The antibonding features appear in the energy range 0.5 to 2 eV, where Co $3d$ contributions are dominant. This suggests that the feature B in Fig. 1 has dominant Co $3d$ character and the intensities corresponding to Si $3p$ photoemission contribute to feature A. The dominance of Co $3d$ contributions in this whole energy range shown presumably leads to unchanged spectral lineshape with the change in photon energy as observed in Fig 1(a) and 1(b).

In order to compare the experimental spectrum with the calculated results, we have calculated the XP spectrum in the following way: the Ce $5d$, Ce $4f$, Co $3d$ and Si $3p$ PDOS per formula unit were multiplied by the corresponding photoemission cross sections at Al $K\alpha$ energy. The sum of all these contributions was convoluted by the

Fermi distribution function at 20 K and broadened by the Lorentzian function to account for the photo-hole lifetime broadening. The resolution broadening is introduced via further broadening of the spectrum by a gaussian function of $\text{FWHM} = 0.4$ eV.

The calculated spectrum is shown by dashed line in Fig. 1(a) after normalizing by the total integrated area under the curve. The intensities near ϵ_F in the experimental spectrum appears to be captured reasonably well in the calculated spectra. In the higher binding energy region, the intensity around 1 eV is overestimated and that around 2.5 eV is underestimated (see Fig. 1). Since this energy range contains dominant contribution from the Co 3d states, it naturally indicates that Co 3d PDOS region is not well described and correlations among Co 3d electrons may be important in determining the electronic structure in this energy range. In order to verify this, we have calculated the electronic density of states considering finite electron correlation, U_{dd} , among Co 3d electrons. The spectral functions corresponding to different U_{dd} values are calculated from the LDA+ U results following the procedure described above.

The lines in Fig. 4 represent the spectral functions for different U_{dd} values which are superimposed on the experimental XP spectrum represented by open circles. In Fig. 4(a) we show the calculated spectra without Ce 4f contributions and the ones including Ce 4f contributions are shown in Fig. 4(b). It is evident from the figure that the signature of the feature around 2.3 eV (feature A) becomes more and more prominent with the increase in U_{dd} . Consequently, the intensity of feature B reduces. Thus, the feature A can be attributed to the photoemission signal from electron correlation induced Co 3d bands (lower Hubbard band) in addition to the Si 3p contributions. It is to note here that although the feature A has comparable contributions from Co 3d and Si 3p states from band structure calculations, the photoemission intensity from the Co 3d states would be larger than that of Si 3p states at XPS photon energies due to the matrix element effects.

It is clear that the calculated spectral functions corresponding to $U_{dd} \sim 3$ eV is close to the experimental spectrum compared to all other cases. For higher values of U_{dd} , the correlation induced feature becomes stronger and appears at higher binding energies. The finding of such correlation among Co 3d electrons is not unrealistic as it is often found in the literature that Co 3d electrons are quite strongly correlated [18, 19, 20, 21, 22]. It is to note here that the estimation of U_{dd} obtained within the LDA+ U calculations in this study suggests signature of significant correlation among Co 3d electrons. An accurate estimate of U_{dd} requires further study using other methods e.g. LDA+DMFT.

The comparison of Fig. 4(a) and 4(b) establishes that the intensities near ϵ_F essentially arise due to the photoemission from the occupied part of the Ce 4f band. The electron correlation among the Co 3d electrons has negligible influence on the spectral intensity at ϵ_F . Consideration of Ce 4f bands in the spectral function calculation leads to a better description of the spectral intensities at the Fermi level. Electron correlation among Ce 4f electrons is also known to be strong. Thus, we verify if such an effect leads to significant spectral intensity at higher binding energies. We show the Ce 4f

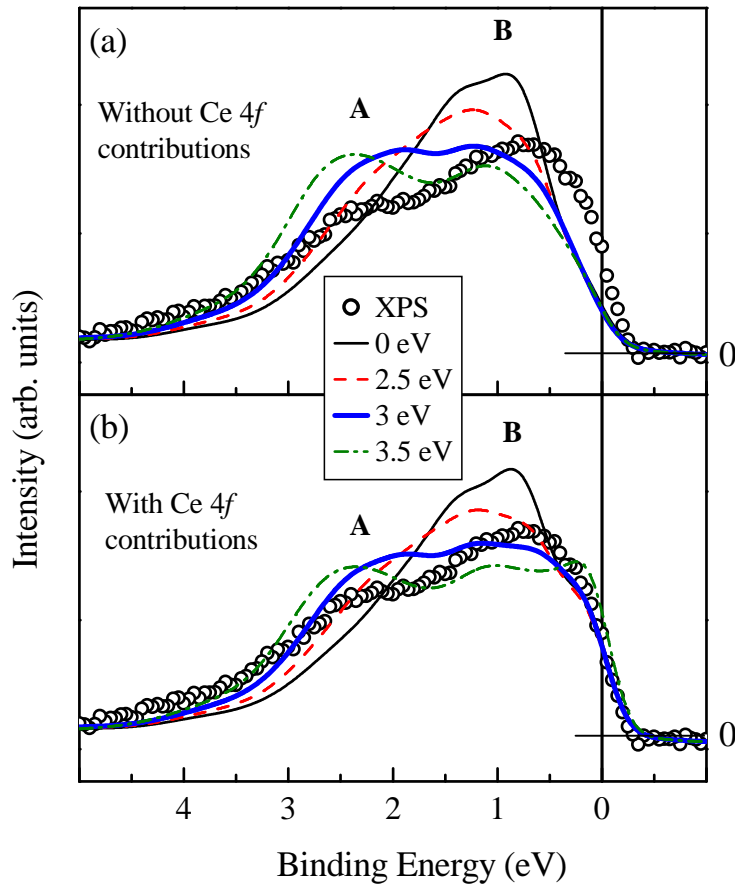


Figure 4. X-ray photoemission valence band spectrum (open circles) is compared with the calculated spectral functions corresponding to different U_{dd} -values. (a) The calculated spectral functions without Ce 4f contributions. (b) The calculated spectral functions contains Ce 4f contributions. Clearly, the results in (b) provide better description than that in (a) revealing signature of Ce 4f contributions in the vicinity of the Fermi level.

PDOS calculated for $U_{ff} = 0$ and 4 eV in Fig. 5. The unoccupied part of the spectral function exhibits large spectral redistribution. The occupied part exhibits a change in lineshape close to the Fermi level as shown with better clarity in Fig. 5(b). Evidently, the 4f contributions appear essentially in the vicinity of the Fermi level even if the 4f correlations are considered.

The signature of electron correlations can also be observed in the Co 2p core level spectra [18, 20, 23]. In Fig. 6, we show the Co 2p spectrum collected at 20 K using Al $K\alpha$ radiation. The spectrum consists of two spin orbit split features Co 2p_{3/2} and Co 2p_{1/2} at 778 eV and 792.9 eV binding energies, respectively (energy separation of about 14.9 eV). These binding energies are identical to those found in elemental Co metals

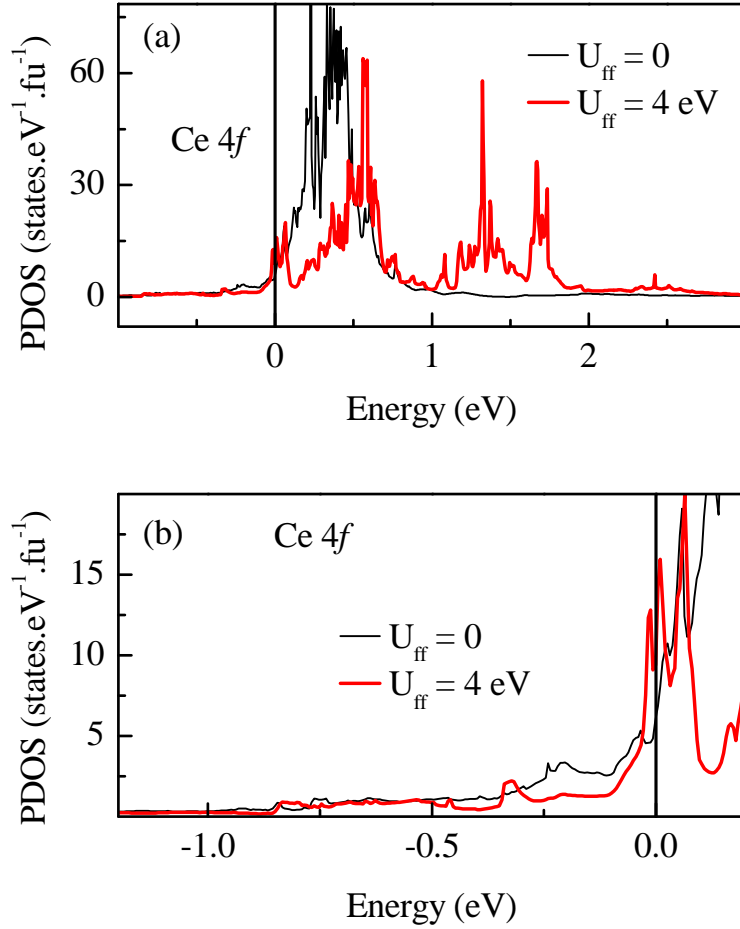


Figure 5. Calculated Ce 4f partial density of states for different electron correlation strength, U_{ff} among Ce 4f electrons. The results corresponding to the whole energy range is shown in (a) and that near Fermi level is shown in (b).

[24, 25]. This indicates that the valence state of Co in this material is very similar to that of the elemental Co metals. In addition, every spin orbit split feature exhibits a weak but distinct shoulder at higher binding energies. This has been shown more clearly by rescaling and shifting this energy region in the same figure. Although the satellite intensity looks small, it appears to be quite intense compared to the ones observed in earlier studies [24, 25]. The energy separation between the main peak and the satellite is about 4 eV.

It is well known that the core level spectra reveal multiple features representing differently screened final states. The intense feature at lower binding energy is usually called the well screened feature and the ones at higher binding energies are called poorly screened features/satellites. Such satellites appear due to the finite electron correlations. The finite intensity of the satellite feature in the present case, independently establishes the presence of electronic correlations among Co 3d electrons as concluded from valence

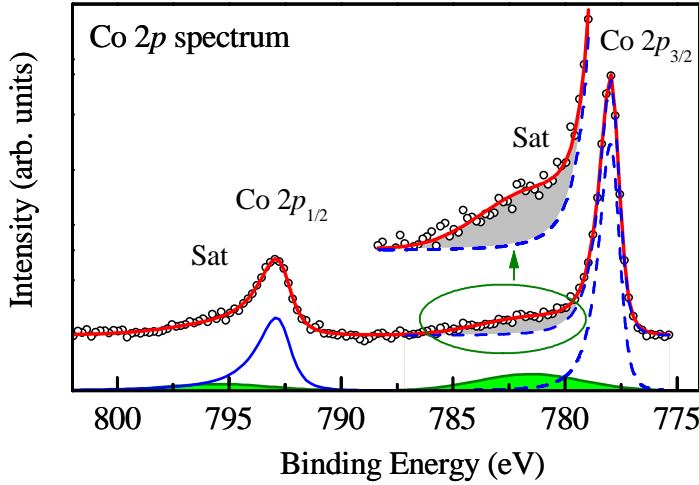


Figure 6. Co 2*p* spectrum (open circles) exhibiting distinct signature of main and satellite peaks. The satellite intensity is shown by shaded region. Solid line passing through the experimental data represents the fit comprising of a main peak (dashed line) and a satellite (shaded peak).

band spectra [23]. Thus, our results establish that the electron correlation strength among Co 3*d* electrons are significant and needs consideration to derive the electronic structure of these systems.

The mixed valency and/or Kondo effect in this class of compounds depends on the Kondo coupling strength, $J \sim \frac{V_{cf}^2}{\epsilon_{4f}}$, where V_{cf} is the hybridization strength between conduction and the 4*f* electronic states, ϵ_{4f} is the binding energy of the 4*f* electrons. In the present case, Co 3*d* electrons contribute significantly in the formation of the conduction band.

Electron correlation introduces local character among 3*d* electronic states; the band dispersion will be weaker than the case without electron correlation and hence the hybridization strength will be weaker. In addition, the formation of the lower Hubbard band at higher binding energies relative to the uncorrelated band due to the electron correlation will influence the effective energy separation between the Ce 4*f* band and the conduction electrons. Thus, J and various hopping parameters involving Co 3*d* electronic states are expected to reduce leading to an effective reduction in the degree of mixed valency of Ce. A quantitative estimation of such effects requires detailed modeling of this case presumably within the periodic Anderson model. We believe that these results will help to initiate such research by the theoreticians.

5. Conclusions

In summary, we have studied the electronic structure of Ce₂CoSi₃ using high resolution photoemission spectroscopy and *ab initio* band structure calculations. The experimental

results indicate the dominance of Co $3d$ contributions in the valence band. Si $3p$ states appear at higher binding energies (2 - 3 eV). The Ce $4f$ contributions appear essentially in the vicinity of the Fermi level. High resolution employed in this study helped to probe the Kondo resonance feature appearing at the Fermi level.

Although the contribution of the Co $3d$ states at the Fermi level is weak, Co $3d$ states are found to be hybridized with the Ce $4f$ states. The comparison of the experimental results with the calculated ones reveal distinct signature of electron correlation among Co $3d$ electrons. These results suggests that description of the electronic structure and various interesting electronic properties involving Kondo systems requires consideration of correlation among conduction electrons.

6. Acknowledgements

One of the authors S.P., thanks the Council of Scientific and Industrial Research, Government of India for financial support.

References

- [1] Brandt N B and Moshchalkov V V 1984 *Advances in Physics* **33** 373
- [2] Wills John M and Cooper Bernard R 1987 *Phys. Rev. B* **36** 3809
- [3] Gunnarsson O and Jepsen O 1988 *Phys. Rev. B* **38** 3568
- [4] Gunnarsson O, Andersen O K, Jepsen O and Zaanen J 1989 *Phys. Rev. B* **39** 1708
- [5] Gunnarsson O and Schönhammer K 1989 *Phys. Rev. B* **40** 4160
- [6] Gordon R A, Alexander M G, Warren C J, DiSalvo F J and Pöttgen R 1997 *J. Alloys Compounds* **248** 24
- [7] Majumdar Subham, Mahesh Kumar M, Mallik R and Sampathkumaran E V 1999 *Solid State Comm.* **110** 509
- [8] Patil Swapnil, Iyer Kartik K, Maiti K and Sampathkumaran E V 2008 *Phys. Rev. B* **77** 094443; Patil Swapnil, Iyer Kartik K, Maiti K and Sampathkumaran E V condmat-0803.0652
- [9] Lawrence J M, Riseborough P S and Parks R D 1981 *Rep. Prog. Phys.* **44** 1
- [10] Blaha P, Schwarz K, Madsen G K H, Kvasnicka D and Luitz J 2001 **WIEN2k**, An Augmented Plane Wave + Local Orbitals Program for Calculating Crystal Properties (Karlheinz Schwarz, Techn. Universität Wien, Austria), ISBN 3-9501031-1-2
- [11] Yeh J J and Lindau I 1985 *At. Data Nucl. Data Tables* **32**, 1
- [12] Maiti K, Manju U, Ray S, Mahadevan P, Inoue I H, Carbone C and Sarma D D 2006 *Phys. Rev. B* **73** 052508
- [13] Maiti K, Kumar A, Sarma D D, Weschke E and Kaindl G 2004 *Phys. Rev. B* **70** 195112
- [14] Maiti K and Sarma D D, 2000 *Phys. Rev. B* **61** 2525
- [15] Maiti K and Singh R S 2005 *Phys. Rev. B* **71** 161102(R)
- [16] Sekiyama A and Suga S 2002 *Physica B* **312-313** 634
- [17] Ehm D, Hüfner S, Reinert F, Kroha J, Wölffe P, Stockert O, Geibel C and Löhneysen H v 2007 *Phys. Rev. B* **76** 045117
- [18] Chainani A, Mathew M and Sarma D D 1992 *Phys. Rev. B* **46**, 9976
- [19] Wu Z Y, Benfatto M, Pedio M, Cimino R, Mobilio S, Barman S R, Maiti K and Sarma D D 1997 *Phys. Rev. B* **56** 2228
- [20] Saitoh T, Mizokawa T, Fujimori A, Abbate M, Takeda Y and Takano M 1997 *Phys. Rev. B* **55** 4257

- [21] Pandey S K, Kumar A, Patil S, Medicherla V R R, Singh R S, Maiti K, Prabhakaran D, Boothroyd A T and Pimpale A V 2008 *Phys. Rev. B* **77** 045123
- [22] Pandey S K, Patil S, Medicherla V R R, Singh R S and Maiti K 2008 *Phys. Rev. B* **77** 115137
- [23] Imada Masatoshi, Fujimori Atsushi and Tokura Yoshinori 1998 *Rev. Mod. Phys.* **70** 1039
- [24] Nath Krishna G, Haruyama Y and Kinoshita T 2001 *Phys. Rev. B* **64** 245417
- [25] Schneider C M, Pracht U, Kuch W, Chassé A and Kirschner J 1996 *Phys. Rev. B* **54** R15618